Measurement of local structural configurations associated with reversible photostructural changes in arsenic trisulfide films

C. Y. Yang, M. A. Paesler, and D. E. Sayers
Department of Physics, North Carolina State University, Raleigh, North Carolina 27695-8202
(Received 20 April 1987)

Extended x-ray-absorption fine-structure measurements have been made on three reversible and reproducible cycles of thermally annealed and light-soaked amorphous As_2S_3 films. Associated with the light-soaked material are (1) a very small increase in the population of wrong bonds in the first shell, (2) an enlarged As—S—As bond angle with an expansion of As—As distance in the second shell, (3) a larger spread in the distribution of As—S—As bond angles, and (4) an absence of any change in the third As—S shell. From these data, we present the first quantitative correlation between observed local atomic structural changes and measured macroscopic properties that are associated with photodarkening. Our data demonstrate that the photoinduced structural changes mainly involve bonding alterations at S atoms as well as a change in the dihedral angle relationship between adjacent AsS_3 pyramids joined at S atoms.

I. INTRODUCTION

The determination of the atomic structure of amorphous semiconductors has long been a much sought but seldom attained goal. For example, several models have been proposed for the structure of the well-characterized material a-As_2S_3. A whole arsenal of experimental studies,[1] including x-ray and neutron scattering, infrared absorption spectroscopy, viscosity, and nuclear quadrupole resonance have lead to a strong suggestion that glassy (g-) As_2S_3 has a layered structure similar to that of crystalline (c-) As_2S_3 or orpiment. Yet some investigators suggest that scattering data do not provide strong evidence for a layered structure.[2] Alternative structural descriptions of the structure of As_2S_3 in terms of the packing of molecular units have also been suggested. deNeufville *et al.*[3] have proposed a model based on dense random packing of As_4S_6 molecules because they believed that vapor in equilibrium with liquid As_2S_3 derived by melting the bulk glass is composed solely of As_4S_6 molecules. The existence of this molecular structure is questionable, since random packing of As_4S_6 molecules could not be experimentally identified.[4] Another molecular model based on As_4S_4 molecules is supported by Raman, extended x-ray-absorption fine-structure (EXAFS), and diffraction data.[4] Phillips[5] has suggested that "structural units comprised of twenty atoms" are present in As_2S_3 glass. It is clear that as yet there is no complete agreement as to the structure of glassy As_2S_3.

An important factor which contributes to this lack of agreement among the proposed models is the method of preparation. Amorphous As_2S_3 may be prepared by evaporation or quenching from the melt. Indeed our study of the effect of quenching on the structure of stoichiometric bulk glasses has demonstrated[6] that the structure of g-As_2S_3 is not unique. Furthermore, it is now widely realized[4] that the structure of evaporated a-As_2S_3 films differs significantly from the structure of parent bulk As_2S_3 glasses. Also noteworthy is the fact that the structure of a- and g-As_2S_3 can also be varied by thermal-annealing and photoinduced processes. Despite a considerable research effort in the past decade, the origin of the reversible photostructural changes observed in a-As_2S_3 has eluded determination.

Because of their structural flexibility, a-As_2S_3 films and bulk samples exhibit large photoinduced structural changes. These photoinduced phenomena are observed as either irreversible or reversible changes, depending on the previous history of the sample. The reversible changes seen in the films and glasses are fundamentally more interesting, since the irreversible changes can be understood[7–10] in terms of photopolymerization of more molecularlike initial configurations. The reversible changes are regarded as unique characteristics of the amorphous state, but the origin of these structural changes has not yet been established. Even though the physical (photoexpansion) and optical (photodarkening) properties are clearly identified, a number of equivocal mechanisms[7,8,10–13] associated with photostructural changes have been proposed. These may involve bond twisting[8] as opposed to bond breaking;[10,12] short-range order[8,10,12] (SRO) as opposed to intermediate-range order[7,11] (IRO), i.e., intramolecule[8,10] as opposed to intermolecule[11] interactions.

The principal reason for the controversy surrounding the determination of the modifications involved in the photostructural change has been inability of any technique to unambiguously identify significant structural changes associated with the effect. For example, x-ray diffraction studies[8] have shown that the first sharp diffraction peak at low scattering vector ($q \sim 1.3$ Å^{-1}) decreases in intensity and shifts slightly to larger q with photodarkening. The effect of light on this peak suggests changes in structural units with at least one dimension on the order of 6 Å. There are, however, no changes in features of the radial distribution function at

this distance. In essence, the structural significance of the low q peak is uncertain.[2] Other qualitative evidence of reversible structural changes has been obtained in Raman studies,[10] but direct and quantitative structural interpretation of these data has not been made.

We take another approach to the study of photostructural changes by using x-ray-absorption spectroscopy (XAS). The XAS technique has become a powerful tool for probing the atomic structure—as well as the electronic and vibrational properties—of a wide range of materials. With recent availability of strong and stable synchrotron radiation sources, the quality of XAS data has dramatically improved so that weak signals from second or even higher shells can be resolved in amorphous solids. In parallel there have been improvements in the data analysis that have made it possible to obtain considerably more accurate information from the experimental data than previously possible. For example in experimental studies of a-As_xS_{1-x} compounds, we have shown[6,9] that EXAFS yields important information about structural disorder, local vibrational motion, and the type of chemical bonding beyond the second shell. Changes in the x-ray-absorption near-edge structure (XANES) between thermally annealed films and photodarkened films have been reported.[9] These changes provide key information about antibonding states associated with the photodarkening phenomena.

II. EXPERIMENTAL PROCEDURE

The a-As_2S_3 films were prepared by evaporating high-purity (99.9999%) pure bulk As_2S_3 glasses. Films were deposited at a rate of 80 Å/sec in a base vacuum of 1×10^{-6} torr onto room-temperature Kapton substrates. Annealing involved heat treatment at 220 °C for two hours while light soaking entailed exposure to an Ar laser beam (488 nm and 500 mW/cm^2) for 5 hours at 77 K. An irreversible change was observed (in EXAFS and ir spectra) upon completion of cycles of annealing, light soaking, and annealing. Three repeated cycles, however, exhibited reversible and reproducible changes. A reversible red shift of the optical edge (i.e., photodarkening) in light-soaked films was confirmed by optical transmission measurements as shown in Fig. 1. Transmission ir spectra were measured from 100 to 800 cm^{-1} and showed no evidence of photo-oxidation.

The XAS spectra performed on the K edge of As were measured at the National Synchrotron Light Source (NSLS) on the X-11 beam line using a double crystal monochromator with Si(111) crystals. The thickness of the films was typically 3.6 μm. Various thicknesses were measured in order to avoid thickness effects. The thicknesses of the samples were also determined by statistical considerations which optimize the signal to noise. Six layers were used to make samples of sufficient x-ray absorption thickness for the EXAFS measurements. Transmission measurements on each sample were made at 80 and 300 K. Four spectra were taken on each sample and were consistent in each series.

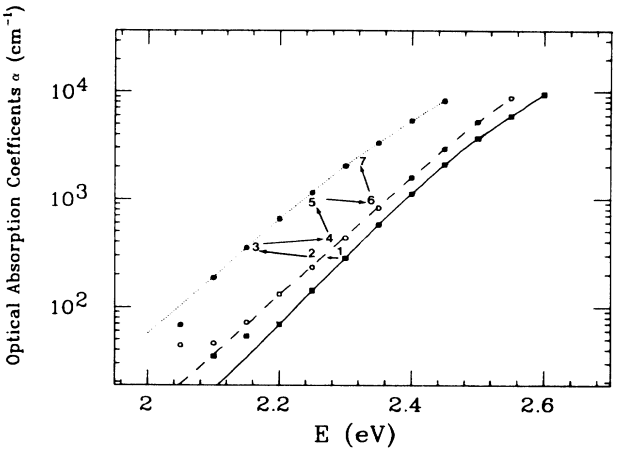

FIG. 1. Optical-absorption edges for virgin (solid line), annealed (dashed line), and light-soaked (dotted line) a-As_2S_3 films. The symbols represent the experimental data. Each cycle is indicated by an arrow. The reproducible and reversible photodarkening was observed in light-soaked films in each cycle. The measurements were performed at room temperature.

III. DATA ANALYSIS AND RESULTS

The K edge of the normalized EXAFS (Ref. 6) can be described by

$$\chi(k)=-\sum_i A_i(k)\sin[2kR_i+\varphi_i(k)] , \quad (1)$$

where the summation extends over i coordination shells at average distance R_i from the absorbing atom, k is the photoelectron wave vector, and $\varphi_i(k)$ is the total phase shift due to contributions from both the absorbing and the backscattering atoms. The amplitude function $A_i(k)$ is given by

$$A_i(k)=(N_i/kR_i^2)F_i(k)\exp(-2\sigma_i^2k^2)\exp(-2R_i/\lambda) , \quad (2)$$

where N_i is the average number of scatterer atoms, $F_i(k)$ is the backscattering amplitude characteristic of a particular type of scattering atom, σ_i^2 is the Debye-Waller factor to account for thermal vibrations $\sigma_i^2(T)$ and static disorder σ_i^2s, and λ_i is the mean-free path of the photoelectron.

The frequency of the EXAFS in Eq. (1) is governed by the radial distance and phase shift. An examination of Eq. (2) shows that the shape of the EXAFS envelope is a function of the number of scatterers N, the backscattering factor $F(k)$, and the Debye-Waller factor $\exp(-2\sigma^2k^2)$. Both the backscattering factor and phase shift depend on the atomic number Z. In the binary As-S system,[14] the backscattering factor of the low-Z atom (the sulfur) is dominant at low k and diminishes rapidly at high k, while the high-Z atom (arsenic) has a small backscattering factor at low k, but large amplitude at high k in comparison with the S atom. Furthermore, the difference in phase shift between As-S and As-As

scattering is approximately π radians. Therefore, the combined features of backscattering amplitude and phase functions can be used to distinguish the species of neighboring atoms (As and/or S) through examination of the k dependence of the EXAFS.

Standard techniques[6] were employed to extract the EXAFS interference function $\chi(k)$ from the overall absorption spectrum. In each of three cycles, both well-annealed and light-soaked films showed reproducible EXAFS spectra with very small uncertainty in the high-k part of the spectrum. Data on the first cycle (i.e., the irreversible effect) are presented elsewhere.[14] In Fig. 2 we presented the $\chi(k)$ data multiplied by k^3 for c-As_2S_3, and thermally annealed and light-soaked amorphous films of the second (line with crosses) and the third (solid line) cycles.

Because $\chi(k)$ is principally a sum of sinusoidal terms, Fourier transforms (FT's) of the data to an R-space representation can separate the contributions from different coordination shells. By using a phase-corrected FT (PCFT),[9] it is possible to identify different types of scatterers. This method involves transforming the EXAFS spectrum after multiplying the data by $\exp[-\varphi_i(k)]$, where the phase shift function is empirically derived from the appropriate standards, either c-As_2S_3 or c-As. The FT's are displayed as the imaginary part which contains amplitude and phase information as well as the magnitude. The As-S PCFT k^3 weighted over a k-space range from 2–16 $Å^{-1}$ shown in Fig. 3 gives positive peaks in the imaginary part for As—S bonds and negative peaks for As—As bonds. In a like manner, the As-As PCFT results[14] in negative peaks in the imaginary part for As—S bonds and positive for As—As bonds.

In Fig. 3, the As-S PCFT shows that the first peak of

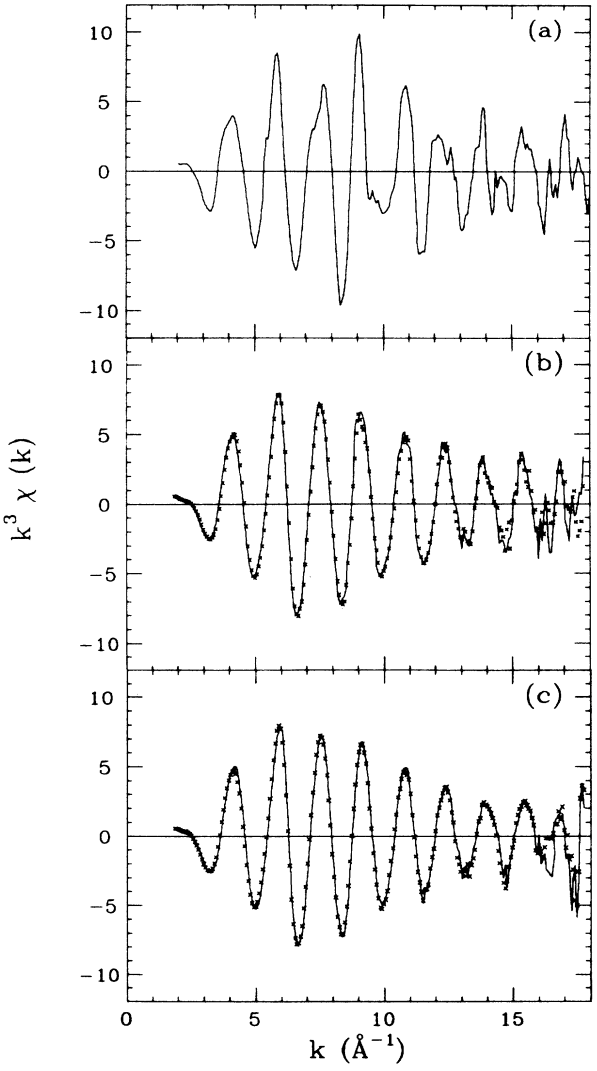

FIG. 2. EXAFS $k^3\chi(k)$ at 80 K for (a) c-As_2S_3, (b) second (line with crosses) and third (solid line) cycles of annealed a-As_2S_3 films, and (c) second (line with crosses) and third (solid line) cycles of light-soaked a-As_2S_3 films.

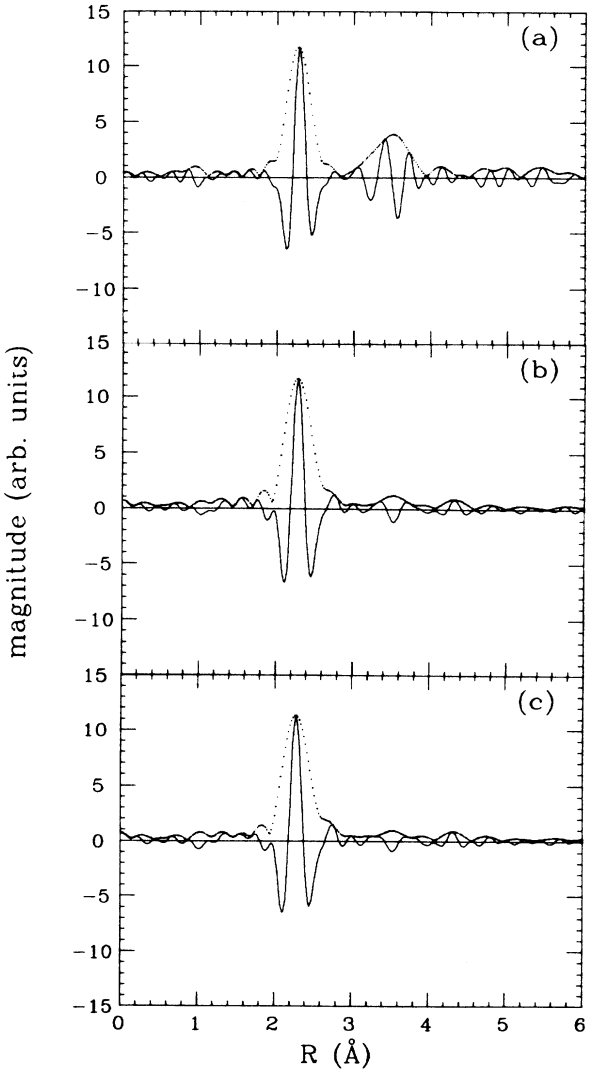

FIG. 3. The As-S PCFT corresponding to Fig. 2 for the imaginary (solid line) and magnitude (dotted line) part of transforms. The k^3 transform was taken over a range of 2–16 $Å^{-1}$.

c-As_2S_3 represents the nearest neighbor of the As—S pairs at a mean bond length of 2.28 Å.[15] The predominant contributions to the first major peaks of the PCFT for annealed and light-soaked films are also determined by the As—S bonds. An additional feature in the first shell is a small shoulder at 2.58 Å which is noticeably different from the corresponding region of the c-As_2S_3 spectrum—especially in the imaginary part of the signal. These shoulders indicate As—As bonds in both films. The data were Fourier filtered ($\Delta R = 1.24$–2.86 Å) to isolate the first-shell EXAFS as shown in Fig. 4. Using the ratio method[6] with the first shell of c-As_2S_3 as a standard, significant deviations from linearity as a function of k^2 occur near 100 $Å^{-2}$, where either As—As contributions or noise begins to dominate the data. Clearly the latter is not the case because of quality of the data as shown in Fig. 2. This suggests the existence of As—As bonds in both films. Using standard fitting techniques with two shells, however, the results are not uniquely able to provide precise determination of the As-As contributions in these samples. An alternative approach for separating minor As-As contributions is by subtracting the dominant contribution of the As—S bonds from the experimental data. Since the signal of the As—S bonds dominates at values of k less than approximately 10 $Å^{-1}$, a good estimate for the As—S contributions can be found by fitting the inverse data only from 3–8 $Å^{-1}$ using either the ratio or nonlinear least-squares fitting. The resulting parameters are shown in Table I. The third row in Table I shows the effects of statistical noise by analyzing one spectrum of c-As_2S_3 using a second independent spectrum of c-As_2S_3 as a reference. Using these parameters over a k-space range of 2–16 $Å^{-1}$ the calculated As—S contribution was obtained and subtracted from the experimental results. An As-As PCFT was then made on the residual spectra. If only As scatterers remain, the residual As-As PCFT would show in a single peak with a symmetric imaginary part in which the maximum coincides with the maximum of the magnitude of the transform. This is shown in Fig. 5 for both films. The peaks below 1.8 $Å^{-1}$ are due to systematic errors introduced by the analysis procedures, but do not significantly affect the data in the region of the As-As shell.

In the first shell, one of the differences (see Table I) between the two films is an increase in the relative Debye-Waller factor $\Delta\sigma^2$ of the As—S bonds in the light-soaked films. This change in $\Delta\sigma^2$ is related to changes in structural as well as compositional SRO, since the thermal vibrational disorder in $\Delta\sigma^2(T)$ of c- and a-As_2S_3 samples is the same, i.e., the optical bond-stretching frequency[6] of the amorphous films is unchanged (to ± 6 cm^{-1}) after the light-soaking process. In Fig. 5, striking differences can be seen in the amplitude of As—As contributions. These changes are reproducible and reversible in each cycle as is evidenced by an independent analysis of two complete cycles. The evidence of an increase of wrong bonds with light soaking is obtained through examination of the ratio of well annealed and light-soaked films. The comparison of structural parameters obtained from this analysis is shown in Table II. Although it is difficult to unambiguously quantify the number of wrong bonds in annealed and light-soaked films because of the strong correlation between coordination number and Debye-Waller factor, trends in wrong-bond populations can be estimated by comparisons with simple models. For example, comparison with a simulated model (0.5% c-As_4S_4 and 99.5% c-As_2S_3) containing 1.7% wrong bonds suggests that the light-soaked sample has 2.0% wrong bonds while the annealed sample has 1.5%. This conclusion is given added strength when one plots the logarithm of the ratio of the

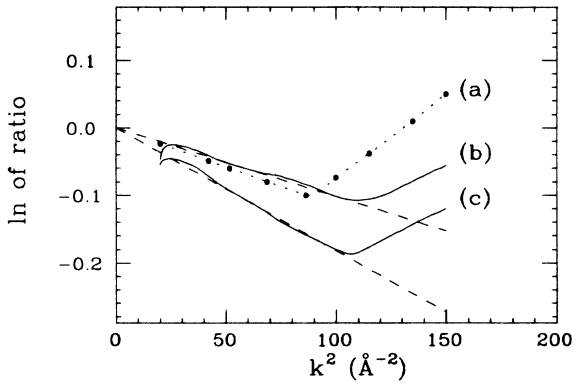

FIG. 4. The ln of amplitude ratio of the first shell plotted vs k^2 for (a) simulated model mixture with 5% of c-As_4S_4 and 95% of c-As_2S_3, (b) annealed films, and (c) light-soaked films. The first shell of c-As_2S_3 was used as a standard in each case.

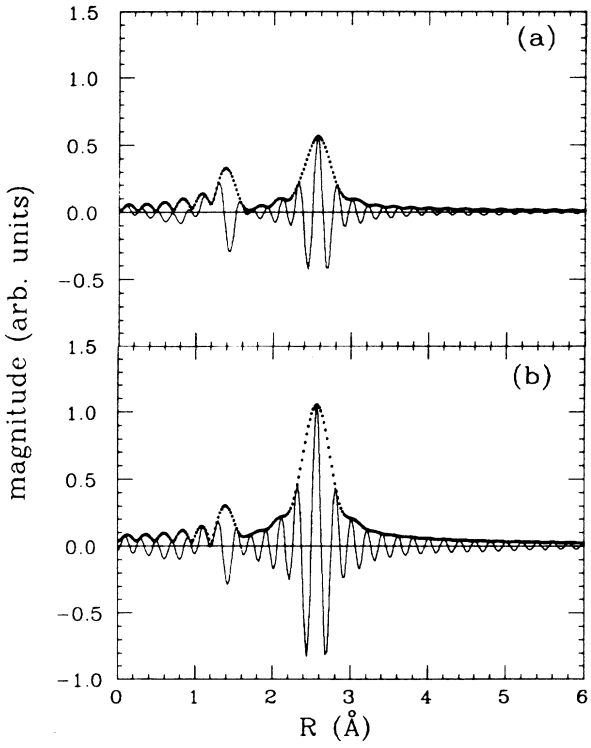

FIG. 5. Residual As-As PCFT for (a) an annealed film and (b) a light-soaked film.

TABLE I. First-shell As-S parameters.

Sample	N	R (Å)	$\Delta\sigma^2 S$ (10^{-4} Å^{-2})	$\Delta\sigma^2(T)$[a] (10^{-4} Å^{-2})
Annealed film[b]	3.0±0.1	2.280±0.003	3.4±1.0	12.1±1.0
Light-soaked film[b]	2.9±0.1	2.280±0.003	5.7±1.0	11.9±1.0
c-As_2S_3[c]	3.00±0.01	2.283±0.001	0.1±0.1	11.0±0.2

[a]$\Delta\sigma^2(T)=\sigma^2(300\text{ K})-\sigma^2(80\text{ K})$.
[b]Noise estimates from different run.
[c]Comparison with c-As_2S_3 measured at 80 K.

amplitude function of g-$As_{42}S_{58}$ and the amplitude function of an annealed film. Because the wrong bond fraction in the g-$As_{42}S_{58}$ is 7%, the intercept of the ratio is ~ 1.62, indicating 1.4% wrong bonds in the annealed films. This compares well with the model-predicted value of 1.5%. The 33% relative increase in coordination number of the As-As first shell is consistent with a change from 1.5% to 2% in going from annealed to light-soaked films. Although we can presently only measure changes in As-As populations, implicit in the creation of As—As bonds at expense of As—S bonds is the creation of S—S bonds.

The second broad peak in the c-As_2S_3 radial structure is complex because of several contributions from intralayer and interlayer S and As neighbors. Because of the large number of parameters involved, it is not possible to quantitatively fit this peak, but because there are large differences between the phase-shift functions and backscattering factors of As and S, then the strong negative peak of the imaginary part in the second major peak of c-As_2S_3 shows that in the EXAFS the shell is dominated by the nonbonding As—As contributions which are influenced by interhelix As—S—As linkages at 3.19 Å and an —As—S—As—S— intrahelix correlation at 3.54 Å. The second peak of radial structural function for amorphous films exhibits *only* a well-defined negative imaginary part which arises from As scattering at 3.48 Å for well-annealed films and 3.50 Å for light-soaked films. We thus conclude that the average second neighbor As—As distances of amorphous films are slightly larger than the mean As—As distance of 3.43 Å in c-As_2S_3.[15] Remarkable is the lack of other contributions to the second shell of the amorphous films. Apparently none of the atomic correlations of the second peak in c-As_2S_3 are retained in the amorphous films. One must keep in mind, however, that both static and dynamic disorder have profound effects on the EXAFS, which means that these other possible atomic correlations are well below detectable limits.

In the second shell, two important differences between annealed and light-soaked films can be noted by examining an expanded view of the As-S PCFT as shown in Fig. 6: (1) the second-neighbor As—As distance is shifted about 0.02 Å in the light-soaked films and (2) the magnitude of the peak in the light-soaked films is reduced from that of annealed films. Difficulties with attempting to determine precise information from the second shell in both films are created by the relatively large Debye-Waller factors. It is possible to determine, however, whether the large variation in the height of the second shell is due to changes in the ordering or due to changes in coordination number, by filtering the second shell EXAFS using an r-space window ($\Delta R = 3.2-3.8$ Å) and comparing the $k^3\chi(k)$ data of both films as shown in Fig. 7. The amplitude envelope of the EXAFS clearly shows the characteristics of the As backscattering function and no sign of any interference effect due to other contributions. This conclusion is also supported by a comparison with the second shell of c-As. The difference of the amplitude envelope between two films can be identified as a function of k. The amplitudes of the spectra are almost identical in the low-k region <5 Å^{-1}, which suggests that the coordination numbers are the same for both films. In the light-soaked films, the amplitude of $\chi(k)$ begins to decrease at $k>5$ Å^{-1} with respect to the annealed films, which suggests that the differences mainly come from the Debye-Waller term. A further comparison shows that the frequency of the spectra changes systematically indicating an increased As-As distance in the light-soaked films.

In Fig. 8, the result of the ratio (dotted line) between the light-soaked and annealed films for the second shell shows a linear fit over a range of k^2 from 9 to 133 Å^{-2}, which extrapolates to $k^2=0$. It is clear that the significant change in the structure of light-soaked films comes from an increase in the structural disorder, since both samples have the same temperature dependence of their Debye-Waller factors. The phase difference (dotted line) between films shown in Fig. 9 indicates the mean As—As bond distance of light-soaked films is shifted

TABLE II. Relative structural parameters for light-soaked films with respect to annealed films. a subscripts denote annealed film.

Shell	Bonding	$\Delta(N-N_a)/N_a$	$\Delta(R-R_a)$ (10^{-2} Å)	$\Delta(\sigma^2-\sigma_a^2)$ (10^{-4} Å^{-2})
1	As—As	0.33±0.11	0.00±0.13	−6.0±4.5
2	As—As	0.00±0.06	2.00±0.12	19.0±2.5
3	As—S	0.00±0.11	0.01±0.14	1.0±4.5

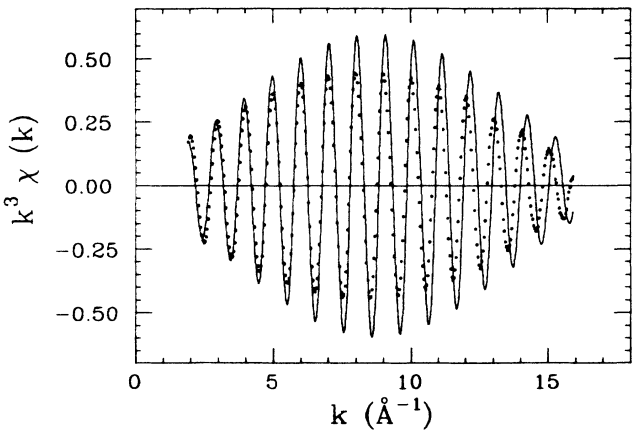

FIG. 6. Comparison of the Fourier filtered EXAFS between the annealed (solid line) and light-soaked films (dotted line) for the second shell. The amplitude envelope of these filtered EXAFS are characteristic of As backscatterers.

0.02 Å toward higher R. The results are listed in Table II. The above results are confirmed by using a nonlinear least-squares fit using the coordination number of the annealed film as a free parameter. A knowledge of the first-neighbor and the second-neighbor bond lengths gives the mean As—S—As angle of 97.5° for c-As_2S_3, 99.5° for annealed films, and 100.3° for light-soaked films, i.e., in the light-soaked films the mean bond angles on S atoms must be opened up 0.8° in order to account for the increase in the mean As—As distance. The increase of structural disorder in the second shell can be easily introduced via bond bending and rotation of the pyramidal units with respect to one another. Using a simple relationship[6,16] between the structural disorder and bonding-angle spread, we find a change in the deviation of the S bond angle about its average of about ±1.8° in the light-soaked films with respect to that of the annealed films. Based on above EXAFS results, it is clear that changes in the second shell upon light-soaking are due to the changes in the As—S—As bond angle accompanied by an expansion of the mean As—As distance.

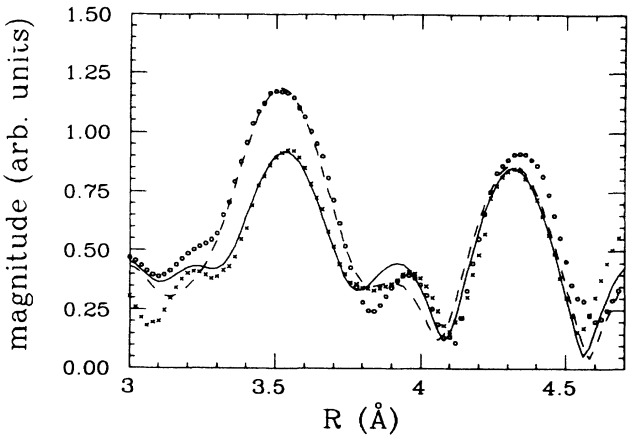

FIG. 7. Expanded view of the As-S PCFT for the second (open circles) and third cycle (dashed line) of the annealed films and the second (line with crosses) and third cycle (solid line) of the light-soaked films. This is to demonstrate the reproducibility and reversibility of photostructural changes in the second- and third-shell contributions.

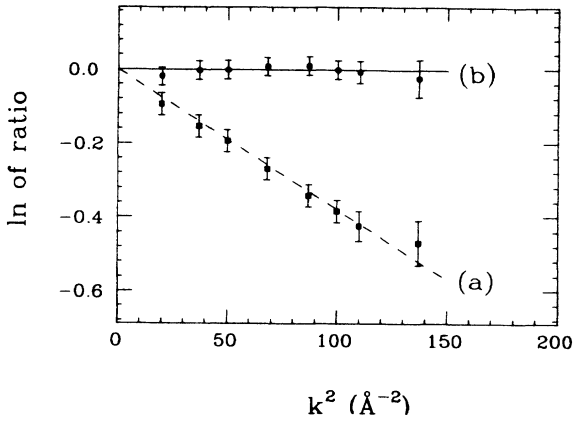

FIG. 8. The ln of amplitude ratio between light-soaked and annealed films for (a) the second shell (dashed line) and (b) the third shell (solid line).

Another interesting feature of c-As_2S_3 is observed in the third peak at 4.10 Å. This small feature arises from S atoms in an —As—S—As—S— spiral chain which is one of the characteristics of the structure of c-As_2S_3. The third well-defined peaks of both films have a maximum at 4.28 Å, suggesting the existence of IRO. Figures 8 and 9 also show the results of ratio and phase difference comparisons for the third shell and demonstrate very little difference between the structure of the light-soaked and annealed films. These results are also listed in Table II.

Other EXAFS experiments have been reported by Elliot[12] and Lowe and Elliot[13] on photostructural changes in g-As_2S_3. Our studies differ from these in several fundamental ways. First, the reversibility of the photostructural changes (as demonstrated in our Fig. 6)

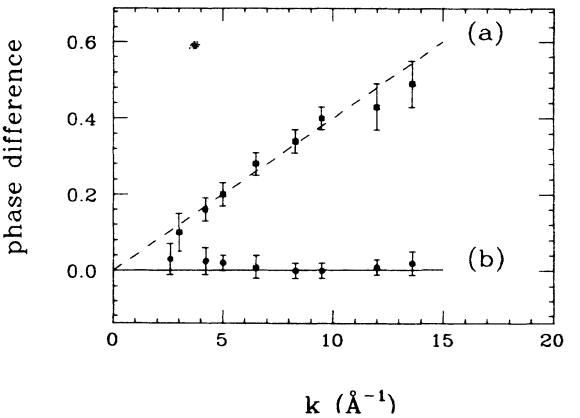

FIG. 9. The ln of phase-difference ratio between light-soaked and annealed films for (a) the second shell (dashed line) and (b) the third shell (solid line). The phase difference corresponds to Fig. 8.

is not evident in earlier works. Indeed the samples studied[13] were said to exhibit only a "partial return to the annealed state." Second, their earlier reports[12,13] of photostructural changes in chalcogenide glasses have shown similar features but have been interpreted differently. Whereas these workers contend that changes in the As-As subshell are below the detectable limits of EXAFS, we have shown that changes in the subshell can be measured and quantified. For illuminated samples Elliot[12] suggested that As—S bonds are transformed into S—S bonds, whereas we have shown that both As—As and S—S bonds must be created. Third, we used filtering techniques to extract quantitative structural information from our data, while Lowe and Elliot[13] felt they could not resolve separate contributions to the second shell, thus obviating quantitative conclusions. Finally, they suggest the possibility of an increase of interlayer separations (As—S) in the second shell to reinforce their particular model. However, the nearest interlayer correlation of As—S contributions is totally missing in our EXAFS data because of the weaker interlayer interaction and the lower vibrational frequency modes which allow a larger relative displacement. Furthermore, in Refs. 4 and 6 as well as in our current data, no experimental evidence for the existence of interlayer correlation (As—S) in g-As_2S_3 and a-As_2S_3 are reported.

IV. DISCUSSION

In the light of the evidence, discernable photostructural changes in SRO have been identified. Though their formation is energetically unfavorable, evidence[10] of wrong bonds has been frequently reported in a-As-S systems. Since the samples are poor thermal conductors, a laser beam may produce photoinduced and/or thermal effects. It has been suggested[10] that for certain situations photodecomposition, observed in Raman measurements, can be attributed to thermal effects. As a result, the laser beam illumination above the optical band gap can lead to small changes in the bond statistics. Thus wrong bonds are randomly dispersed throughout the matrix. From a phenomenological point of view[7] and from experimental results,[17] it has been inferred that both thermally excited structural changes and reversible photostructural changes were of the same kind. Based on this hypothesis, in the light-soaking processes the a-As_2S_3 films are locally heated to a very high temperature and then immediately quenched to a more disordered metastable state. Even though similar photostructural changes (i.e., an enhancement of compositional disorder of the first shell and an increase of fluctuations of the As—S—As bond angle) are observed in the high-temperature atomic configuration of g-As_2S_3 with respect to that of the well-relaxed state,[6] there is no evidence of an expansion of the As—As distance in the second shell. In other words, an increase in the S bond angles with accompanying expansion of the second-neighbor distance is unique to the photostructural changes induced optically. Resolution of the relative roles of heating and photoexcitation—or a combination of both effects—might be made by examining the kinetics of structural changes. Such dynamical EXAFS experiments are currently underway.

Regarding the reversible photostructural changes involving bond breaking, the dominant mechanism responsible for the effect is attributed to an enlarged and more random spread in the As—S—As bond angle. It is reasonable when discussing the photostructural changes in As-chalcogenide materials to focus one's attention on the chalcogen atoms. The low coordination of chalcogen results in a degree of steric freedom for which different structural modifications are possible. These modifications can result in varying degrees of lone pair hybridization[7] which are related to photodarkening. Also, Tanaka[18] has reported on the temperature dependence of photodarkening for chalcogenide glasses. The empirical relation suggests that chalcogen atom configurations are primarily responsible for the photostructural changes.

A geometrical model of spiral chains in which AsS_3 pyramidal units are connected via shared S atoms can be used to examine the important role of S sites in the photostructural changes of a-As_2S_3 films. An immediate consequence of photodarkening is that the two pyramidal units joined at a particular S site are twisted with respect to each other. This must be the case since the As—S—As angle increases while the second As—S distance remains the same. These light-induced distortions can also be thought of as an alteration of the dihedral angle relationships along —S—As—S— $\cdots$ —As—S—As— helices. Since the distortions represent an increased deviation from the low-energy (more crystalline-like) dihedral angle configurations, they introduce a strain. Consequently, a statistically random spread in the distributions of the As—S—As bond angles may stabilize the structure of light-soaked films. Thermal annealing of amorphous films at the glass transition temperature leads to a recovery process to the initial less-strained amorphous state. The details of the structural rearrangement in IRO cannot yet be specified because of the absence of information about higher shell correlations (which would give information about interlayer and cross-ring correlations) and the lack of EXAFS data on the S atoms.

There is other convincing reason to support the significant role of S sites in the photostructural changes. Two distinct causes of a volume expansion may be inferred from our data as shown in Table II. The 33% change in the number of wrong bonds (1.5–2.0 %) alone would result in a fractional increase[10] in volume of $\Delta V/V = 0.3 \times 10^{-3}$. In the second shell, the 2×10^{-2}-Å increase in As—As distance can be shown to result in a fractional increase of $\Delta V/V = 5.7 \times 10^{-3}$. The total increase in volume fraction from the EXAFS data is therefore $\Delta V/V = 6.0 \times 10^{-3}$ which is exactly what has been measured.[8] Although this precise agreement must certainly be considered somewhat fortuitous, we feel that these data provide the first quantitative correlation between microscopic structural models and changes in measured macroscopic properties associated with photostructural changes in amorphous chalcogenides.

V. CONCLUSION

In this work, we have demonstrated that our EXAFS results provide the first quantitative understanding of the microscopic structural modifications associated with reversible photostructural changes in a-As_2S_3. Measured changes induced by light include (1) an increase in the atomic percentage of wrong (As—As) bonds from 1.5% to 2% in the first shell, (2) an enlargement of the mean As—S—As bond angle by 0.8° with an expansion of the mean As—As distance of 0.02 Å in the second shell, (3) a $\pm 1.8°$ increased spread in the distribution of As—S—As bond angles, and (4) an absence of any change in the third As-S shell. These results imply that the photoinduced change involves a twisting of adjacent AsS_3 pyramids about their shared S atoms as well as an expansion of the As—S—As angle at that shared atom. Our EXAFS data do not yet make it possible to correlate the photoinduced effects with specific intermediate range structures. We have, however, shown that associated with the change is an altered dihedral angle relationship centered on the S atoms joining two AsS_3 pyramids. In order to obtain a deeper insight into IRO structures that may be involved with photodarkening, we are currently merging other experimental techniques such as x-ray scattering and Raman spectroscopy with structural modeling on these samples. By coupling our EXAFS results with these other data and structural models, we hope to ascertain more completely the intermediate-range structural modifications associated with photoinduced changes in a-As_2S_3.

ACKNOWLEDGMENTS

We are grateful to J. M. Lee and G. Pfeiffer for assistance with sample preparation and optical measurements. This work was supported by U.S. Department of Energy Contract No. DE-AS05-80ER10742 and NSF Grant No. DMR-8470265.

[1]L. E. Busse, Phys. Rev. B **29**, 3639 (1984), and references therein; M. Rubinstein and P. C. Taylor, *ibid.* **9**, 4258 (1974), and references therein.

[2]A. C. Wright, R. N. Sinclair, and A. J. Leadbetter, J. Non-Cryst. Solids **71**, 295 (1985).

[3]J. P. deNeufville, S. C. Moss, and S. R. Ovshinsky, J. Non-Cryst. Solids **13**, 191 (1973/1974).

[4]R. J. Nemanich, G. A. N. Connell, T. M. Hayes, and R. A. Street, Phys. Rev. B **18**, 6900 (1978); M. F. Daniel, A. J. Leadbetter, A. C. Wright, and R. N. Sinclair, J. Non-Cryst. Solids **31**, 271 (1979).

[5]J. C. Phillips, J. Non-Cryst. Solids **43**, 37 (1981).

[6]C. Y. Yang, D. E. Sayers, and M. A. Paesler (unpublished); C. Y. Yang, M. A. Paesler, and D. E. Sayers, Mater. Lett. **4**, 233 (1986); C. Y. Yang, D. E. Sayers, and M. A. Paesler, in *National Synchrotron Light Source Annual Report* (Brookhaven National Laboratory, New York, 1985), p. 203.

[7]J. P. deNeufville, in *Optical Properties of Solids—New Developments,* edited by B. O. Seraphin (North-Holland, Amsterdam, 1975), p. 437, and references therein.

[8]Ka. Tanaka, in *Amorphous Semiconductors: Technology and Devices,* edited by Y. Hamakawa (North-Holland, Amsterdam, 1982), p. 227, and references therein.

[9]D. E. Sayers, C. Y. Yang, and M. A. Paesler, in *Disordered Semiconductors,* edited by M. Kastner, G. A. Thomas, and S. Ovshinsky (Plenum, New York, 1987); C. Y. Yang, D. E. Sayers, J. M. Lee, and M. A. Paesler, Bull. Am. Phys. Soc. **31**, 381 (1986); C. Y. Yang, J. M. Lee, D. E. Sayers, and M. A. Paesler, J. Phys. Paris (Colloq.), **47**, C8-387 (1986).

[10]A. E. Owen, A. P. Firth, and P. J. S. Ewen, Philos. Mag. **52**, 347 (1985), and references therein.

[11]S. R. Elliot, J. Non-Cryst. Solids **81**, 71 (1986).

[12]S. R. Elliot, J. Non-Cryst. Solids **59/60**, 899 (1983).

[13]A. J. Lowe and S. R. Elliot, Philos. Mag. **54**, 483 (1986).

[14]C. Y. Yang, Ph.D. dissertation, North Carolina State University, 1987 (unpublished).

[15]D. J. E. Muller and W. Nowacki, Z. Kristallogr. **136**, 48 (1972).

[16]M. A. Paesler, D. E. Sayers, R. Tsu, and J. G. Hernandez, Phys. Rev. B **28**, 4550 (1982); C. E. Bouldin, Ph.D. dissertation, University of Washington, 1984.

[17]K. Kimura, H. Nakata, K. Murayama, and T. Ninomiya, Solid State Commun. **40**, 551 (1981).

[18]Ke. Tanaka, J. Non-Cryst. Solids **59&60**, 925 (1983).